

## Novel method of small target detection in infrared images\*

CUI Yu-ping, LIU Yong-cai

(Key Laboratory of Education Ministry for Image Processing and Intelligent Control Institute for Pattern Recognition and Artificial Intelligence, Huazhong University of Science and Technology, Wuhan 430074, China)

**Abstract:** Based on the characteristic analysis of infrared naval vessel target under the sea-sky background, a new adaptive infrared small target detection method is developed, which uses the LOG operator to detect the outline of the target and then decides its center point as the seed point in the region growing procedure. In the proposed approach, the parameters of the LOG operator are adaptively determined using the roughness estimation of the background. This procedure is a preprocessing method of the detection and recognition of the small target, and it can reduce the computation requirement, improve the detection speed, restrain the unnecessary seed points in region growing process, and increase the possibility of target detection.

**Key words:** Small target detection and segmentation; LOG operator; Roughness of the background; Region growing

**CLC number:** TP391 **Document code:** A **Article ID:** 1007-2276(2005)05-0587-05

## 新的红外图像小目标检测方法\*

崔玉平, 刘永才

(华中科技大学模式识别与人工智能研究所 图像处理与智能控制教育部重点实验室,  
湖北 武汉 430074)

**摘要:** 在分析了海空背景下舰船目标红外图像特征的基础上, 提出了一种基于背景粗糙度估计的红外图像小目标自适应检测算法, 该算法利用 LOG 算子检测目标的大致轮廓, 确定目标的中心点作为区域生长的种子点, 可以看作是为后续处理压缩数据量的一种方法。它可以减少运算量, 提高检测速度, 抑制对不必要的种子点的区域生长, 提高目标的检测概率。

**关键词:** 小目标检测与分割; LOG 算子; 背景粗糙度; 区域生长

### 0 Introduction

Target detection technique, based on a single frame infrared image, directly detects the infrared target

from the single frame image by using the various characteristics of the target itself or the background. To detect the target by using the differences between the target itself and the background, the key is to extract

收稿日期: 2004-12-10; 修订日期: 2005-02-01

\* 基金项目: 武器装备预先研究基金(51476040304JW0508)

作者简介: 崔玉平(1964-), 男, 河南鄆城人, 所长, 高级工程师, 博士, 主要研究方向为光学系统设计, 图像识别与智能系统等。

the characteristics of the target or the background. The detection and recognition method greatly depends on the size and the relative area of the target itself. Generally, the area target has geographic information, and its detection approach relies on area ratio of the target to the background. For the spot or small target, an effective approach is to analyze the noisy intensity of the background<sup>[1-4]</sup>, which is called roughness of the background in this paper.

Based on the characteristic analysis of infrared naval vessel target under the sea-sky background, this paper is to explore a new adaptive infrared small target detection method, which uses the LOG operator<sup>[5]</sup> to detect the outline of the target and then decide its center point as the seed point in the region growing procedure.

## 1 Fast background roughness-based target detection algorithm

The proposed algorithm includes roughness estimation of the background, and uses the LOG operator to detect the outline of the target, and decides center points as the seed point in the region growing process and the target segmentation sub-procedures.

### 1.1 Review of the LOG operator

The edges in an image usually refer to rapid changes in some physical properties, such as geometry, illumination and reflectivity. Mathematically, a discontinuity may be involved in the function representing such physical properties. Most edge detectors, such as the gradient-based methods or zero-crossing approaches, require convolving an image with a kernel to compute gradients or zero-crossings. Based on the result of the convolution, a decision is then made as to whether a pixel is an edge or not. The gradient-based methods give very little control over image noise and edge location. The second-order derivative approach tends to exaggerate noise twice as much. Some sort of noise suppression is needed. The LOG operator uses the

Gaussian filter to serve the purpose of smoothing for noise reduction. The image is firstly smoothed with the following Gaussian function:

$$G(x, y, \sigma) = \frac{1}{2\pi\sigma^2} \exp\left(-\frac{1}{2\sigma^2}(x^2 + y^2)\right) \quad (1)$$

Where the  $G(x, y, \sigma)$  is a circle symmetric function, the  $\sigma$  controls the smoothing strength. Mathematically, the smoothing procedure is a convolving operation,

$$g(x, y) = G(x, y, \sigma) * f(x, y) \quad (2)$$

where  $(x, y)$  is the original image,  $g(x, y)$  is the smoothed image. Marr uses the Laplacian operator to detect the zero-crossing of the second-order derivatives, that is

$$\begin{aligned} \nabla^2 G(x, y) &= \nabla^2((G(x, y) * f(x, y))) = \\ &= (\nabla^2 G(x, y, \sigma)) * f(x, y) \end{aligned} \quad (3)$$

where  $\nabla^2 G$  is the LOG operator:

$$\begin{aligned} \nabla^2 G(x, y, \sigma) &= \frac{\partial^2 G}{\partial x^2} + \frac{\partial^2 G}{\partial y^2} = \frac{1}{\pi\sigma^4} \left( \frac{x^2 + y^2}{2\sigma^2} - 1 \right) \times \\ &= \exp\left(-\frac{1}{2\sigma^2}(x^2 + y^2)\right) \end{aligned} \quad (4)$$

In practice, to reduce the computational requirements of the convolution operation,  $\nabla^2 G$  is usually approximated by the differences of the two Gaussian bent surface with different bandwidth. Then the LOG operator can be rewritten as follows<sup>[7,8]</sup>:

$$\nabla^2 G = k \left( 2 - \frac{x^2 + y^2}{\sigma^2} \right) \exp\left(-\frac{x^2 + y^2}{2\sigma^2}\right) = h_{12}(x, y) + h_{21}(x, y) \quad (5)$$

$$h_{12}(x, y) = h_1(x) h_2(y) \quad (6)$$

$$h_{21}(x, y) = h_2(x) h_1(y) \quad (7)$$

$$h_1(\xi) = \sqrt{k} \left( 1 - \frac{\xi^2}{\sigma^2} \right) \exp\left[-\frac{\xi^2}{2\sigma^2}\right] \quad (8)$$

$$h_2(\xi) = \sqrt{k} \exp\left[-\frac{\xi^2}{2\sigma^2}\right] \quad (9)$$

where  $k$  is a intensity factor, and  $\sigma$  is Gaussian width.

Experiments have demonstrated that the larger the  $\sigma$  in the LOG operator, the fewer the detected edge pixels, which can be explained by the frequency character of the Gaussian filter. As the Fourier transform of the Gaussian function  $g(t, \sigma) = \frac{1}{\sqrt{2\pi}\sigma} \exp(-x^2/2\sigma^2)$  is  $F(\omega, \sigma) = \exp(-\omega^2\sigma^2/2)$ , the Gaussian filter is a low-pass filter. The larger  $\sigma$  means more narrow frequency bandwidth, which greatly reduces the high-frequency noise and avoids to detect the false edges. It is worth noting that the some edges can't be detected since the Gaussian filter simultaneously smoothed the edges and the noises. To solve the contradiction between the noisy reduction and the precise edge location, the basic idea is to adaptively decide the  $\sigma$  of the LOG operator according to the different noisy background. Here, we use the roughness of the background to adaptively decide  $\sigma$  of the LOG operator and then detect the edges.

## 1.2 Estimation of the roughness of the background

From the discussion mentioned above, we can draw the conclusion that the key of the LOG edge detector is to decide the suitable Gaussian width  $\sigma$  and the intensity factor  $k$ . Unsuitable configuration of these parameters may significantly reduce the effectiveness of the proposed method. For the sea-sky background infrared image, the main noise is from the sea miscellaneous wave, which is the main factor of influence the extraction of the outline of the target. To restrain the sea miscellaneous noise and extract the available information, the roughness of the natural object is used to describe the intensity of the sea miscellaneous wave and determine the two parameters of LOG operator. How to determine the parameters of LOG operator according to the roughness of the practical sea-sky infrared images is the key for the proposed method. The larger roughness of the background, the larger the  $\sigma$  and the smaller the  $k$ , and vice versa.

To estimate the roughness of the practical sea-sky infrared images, it is important to analyze the possible

factors that determine the roughness. The infrared information in an infrared image represents the flux of the infrared radiation of the scenery. For the sea-sky background infrared image, it is mainly from the sea miscellaneous wave. Cox and Munk proposed that the sea miscellaneous wave can be partitioned into planar facets, and introduced slope distributions on two directions. As the reflectivity, emissivity and slope of the facet decide that the detector can detect the reflection from which parts of the sky and clouds, the slope distributions greatly impact the detector's receiving of the infrared radiation. Cox and Munk proposed the slope distribution model of the facets by observing the offing reflections. For every bright light, there must be a facet to reflect the sun-light to the detector. The slope of the facet is determined by the elevation of the sun and the detector, and the azimuth angle between them.

Assume the  $x, y$  present the direction axis of the side wind and tail wind,  $s$  presents the slope of the facet,  $\alpha$  is the azimuth angle of the  $s$  off the  $y$  axis positive direction.  $S_x$  and  $S_y$  respectively represent the slope of the side wind and tail wind direction, that is

$$S_x = s \sin(\alpha) \quad (10)$$

$$S_y = s \cos(\alpha) \quad (11)$$

Cox and Munk deduced the probability function of slope distribution  $S_x$  and  $S_y$  could be approximated by the Gaussian function, that is

$$P(S_x, S_y) = (2\pi\sigma_x\sigma_y)^{-1} \exp\left\{-\left(\frac{S_x^2}{\sigma_x^2} + \frac{S_y^2}{\sigma_y^2}\right)/2\right\} \quad (12)$$

where the  $\sigma_x$  and  $\sigma_y$  are respectively the variances of slope distribution  $S_x$  and  $S_y$ . Therefore  $P(S_x, S_y)dx dy$  represents the probability of the facet with slope of  $S_x \pm dx$  and  $S_y \pm dy$ .

The squared difference of the slope is related with the wind speed, which can be described by the following function

$$\sigma^2 = 0.003 + 5.12 \times 10^{-5}v \quad (13)$$

$$\sigma^2 = \sigma_x^2 + \sigma_y^2 \quad (14)$$

where  $\nu$  is wind speed(cm/s).

For a practical sea-sky background infrared image, the roughness of background can be approximated by the following self-correlative function,

$$C(\varepsilon, \eta, m, n) = \frac{\sum_{m=\varepsilon-L}^{\varepsilon+L} \sum_{n=\eta-L}^{\eta+L} f(m, n) f(m-\varepsilon, n-\eta)}{\sum_{m=\varepsilon-L}^{\varepsilon+L} \sum_{n=\eta-L}^{\eta+L} [f(m, n)]^2} \quad (15)$$

$$T(\varepsilon, \eta) = \sum_{\varepsilon=-L}^L \sum_{\eta=-L}^L \varepsilon^2 \eta^2 C(\varepsilon, \eta, m, n) \quad (16)$$

where  $\varepsilon, \eta = 0, \pm 1, \pm 2 \dots \pm L$  are the departure value, larger roughness results in larger  $T$  value.

In the proposed approach, to optimally extract the outline of the object, the  $\sigma$  and  $k$  value of the LOG operator are adaptively determined according to the roughness ( $T$ ) of the background. The relationship between the  $\sigma$  and  $k$  and the roughness ( $T$ ) of the background is experimentally determined.

### 1.3 Image segmentation based on the region growing

When the outline of the object is extracted from the image, the approximate position of the object can be located and the object can be segmented from the background by using the region growing technique. Region growing, based on the idea that the similar pixel should form a region, is the basic region segmentation method, including single connective region growing, central connective region growing and mixing connective region growing techniques. The basic region growing procedures are listed as follows.

(1) Find a seed pixel in every needing segmental region as the starting point.

(2) Unite the seed pixels' neighborhood pixels being the same character as or similar character with the seed pixels into the region where the seed pixels exist. In this uniting process, the similarity of the pixels should be decided with the predefined growing or similar rule.

(3) Use the new pixels as the new seed pixels, and repeat the second step till there are none pixels satisfying the similar rule.

#### 1.3.1 Selection of the seed pixels

In practice, image segmenting process with the region growing technique, it is important to select suitable seed pixels and end-growing condition. In the proposed method, the seed pixels are the central pixels of the extracted outlines of the objects in the infrared image. Region growing with these selected seed pixels can increase the region growing speed and improve the segmental results, since these nonrandom selected seed pixels locate in the object regions and then the followed region growing only processes in the object regions. Therefore, the proposed approach introduced the central connective region growing technique.

#### 1.3.2 Selection of the region growing threshold

To segment the object from the infrared image, based on the approximate object position obtained by the above mentioned method, a simple and fast region growing threshold selection method is proposed.

Assume the beginning mean gray value of the object is  $\hat{g}_0 = E[f(x, y) | (x, y) \in R_0]$ , where the  $R_0$  is  $5 \times 5$  pixels size region centered at the outline of the object. The mean gray value of the background is  $\hat{g}_b = E[f(x, y) | (x, y) \in R_b]$ , where  $R_b$  are the region with the first  $n$  rows in the sampling region. In the experimental procedure, the  $n$  is set to 8, since the sea and sky backgrounds simultaneously exist and the probability of the first 8 rows in the sampling region being the background is maximum, which is demonstrated by the experiments. In this way, the estimated region growing threshold is  $\hat{T}_0 = \hat{g}_0 + \lambda |\hat{g}_b - \hat{g}_0|$ , where the  $\lambda$  is a adjustable parameter, which is related with the area of the object and background.

## 2 Results and discussions

To demonstrate the effectiveness of the proposed

algorithm, a large variety of computer experiments are carried out. Fig.1(a) and Fig.2(a) are respectively the original naval-vessel infrared images, where the naval-vessel objects are obvious while the sea miscellaneous noises are large. Fig.1(b) and (c), Fig.2(b) and (c) are respectively the results segmented with the Otsu and 2-dimensional entropy methods, and Fig.1(d) and Fig.2(d) show the results segmented with the proposed approach. These results demonstrated that the proposed algorithm is effective.

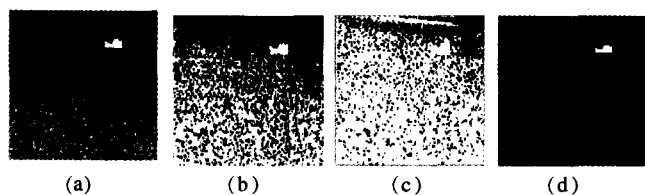


Fig.1 Comparison of the results segmented with different methods



Fig.2 Comparison of the results segmented with different methods

For the small target of the sea-sky background infrared image, the proposed approach uses the approximated roughness of the background to adaptively determine the parameter of the LOG operator, and then uses the central connective region growing technique to segment the target from the background. As the parameters of the LOG are adaptively determined according to the roughness of the background, the contradiction between the noisy reduction and the object location is well solved, the effectiveness of the proposed approach is illustrated by the experimental results.

Since the sea-sky background doesn't rapidly change, the last 20 rows in the bottom with higher noise level to approximate the roughness of the whole background can be used and then the computational requirements can be greatly decreased. At the same time, the central connective region growing technique can signifi-

cantly speed up the object segmenting process. Therefore, the proposed approach can be applied to real-time object segmentation.

### 3 Conclusions

The new fast background roughness infrared naval-vessel target detection algorithm is proposed in this paper, where the parameters of the LOG operator used to extract the outline of the object are adaptively determined according to the roughness of the background. Based on the extracted outline, the object segmentation is completed quickly by using the central connective region growing technique. A large variety of computer experimental results demonstrate that the proposed algorithm is efficient and effective.

### References :

- [1] LUO Ji-qiang, WU Zhen-sen, DONG Yan-bing, et al. New method of IR small dim target detection in big clutter background[J]. *Infrared and Laser Engineering* (罗继强, 吴振森, 董雁冰, 等, 强噪声背景下红外弱小目标的快速检测方法. *红外与激光工程*) 2004, 33(1):47-49, 58.
- [2] Berizzi F, Dalle-Mese E. Scattering from a 2D sea fractal surface: fractal analysis of the scattered signal[J]. *IEEE Trans on Antennas and Propagation*, 2002, 50(7):912-925.
- [3] Glen S Wallinga, Edward J Rothwell, Kun-Mu Chen. Enhanced detection of a target in a sea clutter environment using a stepped, ultra-wideband signal and E-pulse cancellation[J]. *IEEE Trans on Antennas and Propagation*, 2001, 49(8):1166-1173.
- [4] ZHENG Cheng-yong, LI Hong. Method of infrared target detection based on the characteristic analysis of the local grey level[J]. *Infrared and Laser Engineering* (郑成勇, 李红. 基于局部灰度特性分析的红外目标检测方法. *红外与激光工程*), 2004, 33(4):362-365.
- [5] Andres Huertas, Gerard Medioni. Detection of intensity changes with subpixel accuracy using laplacian-gaussian masks[J]. *IEEE Transactions on Pattern Analysis and Machine Intelligence*, 1986, 8(5):651-664.